ACS NANO

Cite This: ACS Nano 2018, 12, 2283−2291

www.acsnano.org

ARTICLE

Glucose Sensing with Phenylboronic Acid Functionalized Hydrogel-Based Optical Diffusers

Mohamed Elsherif,*,† Mohammed Umair Hassan,† Ali K. Yetisen,‡ and Haider Butt*,†

†Nanotechnology Laboratory, School of Engineering and ‡School of Chemical Engineering, University of Birmingham, Birmingham B15 2TT, U.K.

Supporting Information

ABSTRACT: **Phenylboronic acids have emerged as synthetic receptors that can reversibly bind to *cis*-diols of glucose molecules. The incorporation of phenylboronic acids in hydrogels offers exclusive attributes; for example, the binding process with glucose induces Donnan osmotic pressure resulting in volumetric changes in the matrix. However, their practical applications are hindered because of complex readout approaches and their time-consuming fabrication processes. Here, we demonstrate a microimprinting method to fabricate densely packed concavities in phenylboronic acid functionalized hydrogel films. A microengineered optical diffuser structure was imprinted on a phenylboronic acid based *cis*-diol recognizing motif prepositioned in a hydrogel film. The diffuser structure engineered on the hydrogel was based on laser-inscribed arrays of imperfect microlenses that focused the incoming light at different focal lengths and direction resulting in a diffused profile of light in transmission and reflection readout modes. The signature of the dimensional modulation was detected in terms of changing focal lengths of the microlenses due to the volumetric expansion of the hydrogel that altered the diffusion spectra and transmitted beam profile. The transmitted optical light spread and intensity through the sensor was measured to determine variation in glucose concentrations at physiological conditions. The sensor was integrated in a contact lens and placed over an artificial eye. Artificial stimulation of variation in glucose concentration allowed quantitative measurements using a smartphone's photodiode. A smartphone app was utilized to convert the received light intensity to quantitative glucose concentration values. The developed sensing platform offers low cost, rapid fabrication, and easy detection scheme as compared to other optical sensing counterparts. The presented detection scheme may have applications in wearable real-time biomarker monitoring devices at point-of-care settings.**

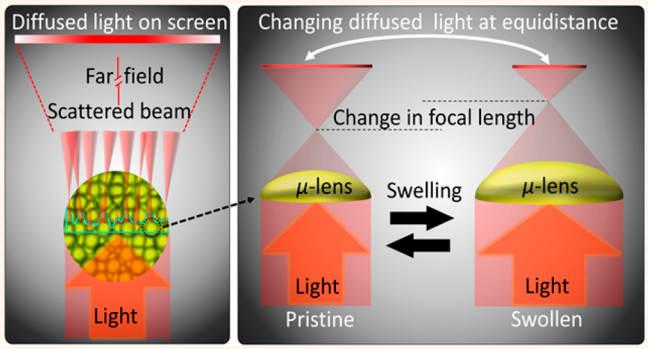

KEYWORDS: *diffraction, photonic microstructures, glucose sensor, phenylboronic acid, contact lenses*

Glucose sensors based on various optical phenomena have been extensively explored. Optical glucose sensors can be classified into four groups according to the optical transducer/phenomena: surface plasmon resonance (SPR), fluorescent, Surface Enhanced Raman Scattering (SERS), and the photonic band gap sensors. For instance, plasmonic sensors were investigated for glucose sensing due to their high sensitivity to the change in the surrounding dielectric constant. The readout of these sensors depended on detecting the change in the resonant absorbed wavelength with glucose concentrations. An enzyme responsive plasmonic nanoshell system was reported to sense glucose through enzyme complexation.[1] Aggregation and dissociation of gold nanoparticles coated with dextran were also utilized to sense glucose. The nanoparticles aggregate with concanavalin A induced by glucose led to a change in plasmonic absorption.[2]

SERS surfaces were adopted for glucose sensing as it enhanced the scattered Raman signal by molecular adsorption and the enhancement factor can reach up to 10^{11} fold.[3] The intensity of Raman spectra can be used to quantify the concentration of glucose. For example, a template of mercaptophenyl boronic acid (MBA) and silver/gold nanoparticles with graphene oxide nanomaterial was developed to enzymatically sense glucose.[4] Gold nanostar silica core−shell nanoparticles were prepared with glucose oxidase as a SERS substrate for label-free glucose detection.[5] In-situ gold nanoparticles were created in porous and stable metal−organic

Received: October 6, 2017
Accepted: March 12, 2018
Published: March 12, 2018

DOI: 10.1021/acsnano.7b07082
ACS Nano 2018, 12, 2283−2291

framework and this system was decorated with glucose and lactate oxidases for *in vivo* detection of glucose and lactate *via* SERS.[6] However, the fabrication of SERS and SPR glucose sensors require high vacuum and advanced technologies such as atomic layer deposition and e-beam deposition, making the process costly and complicated. In addition, the readout methods of both systems require a customized setup of high-cost optical fibers or a Raman spectrometer.

Fluorescent sensors for continuously monitoring of glucose have also been reported. For example, PBA containing fluorophores was employed in a wearable device for continuous glucose monitoring. The employed charge transfer mechanism induced spectral changes in the presence of glucose. The fluorescence wavelength and the intensity shift with glucose complexation.[7] Fluorescent sensors suffer from photobleaching of the fluorophore and variations in the illumination source causes over/underestimation of the glucose concentrations.

Hydrogels of integrated photonic band gap (PBG) structures have been functionalized and designed to undergo a reversible change in their physical dimension in response to external stimuli such as glucose, pH, ionic strength, temperature, humidity, solvent composition, and biomolecule binding.[8−19] The photonic band gap of the hydrogel sensors are sensitive to hydrogel's volumetric change and convert this change into readable optical information. The hydrogel photonic sensors can be classified into three types according to the dimensions of the refractive index periodicity: 1D, 2D, and 3D photonic bandgap sensors. In such sensors, the reading out can be recorded by colorimetric, and spectral shift measurements.[20−27]

Phenylboronic acid functionalized hydrogel is a glucose-responsive system due to their affinity to diol-containing molecules.[8,24] The complexation of PBA immobilized in the hydrogel matrix with glucose molecules causes volumetric change (Figure 1). Self-assembly methods have been utilized for the formation of 3D-PBG structure and 3D inverse opal (IO) PBG structure combined with PBA modified hydrogel for glucose sensing.[28] The PBA functionalized 3D-PBG (IO) hydrogel sensors based on the polymerized acrylamide around 3D sacrificial charged polystyrene particles, have been shown to sense the glucose concentration obeying Bragg's law.[29] Due to their intrinsic periodicity, these 3D-PBG sensors diffract light of certain wavelengths at specific incident angles. Thereby, at a particular point in space, spectral shifts are observed because of the change in the lattice size and periodicity induced by the swelling (or shrinking) of hydrogel sensing the external stimuli.

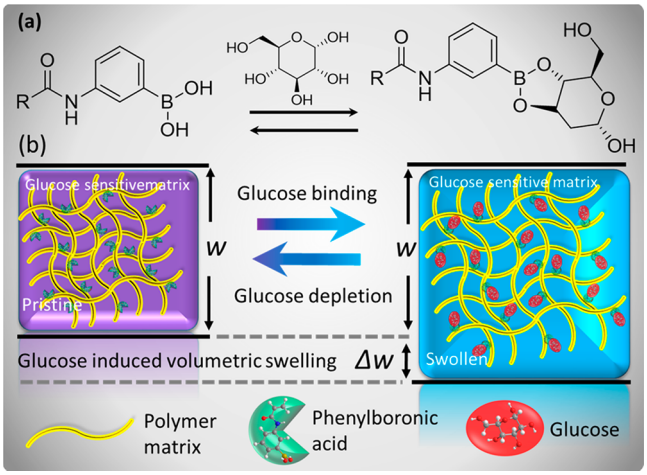

Figure 1. Schematic illustration of glucose-induced swelling of the phenylboronic acid functionalized hydrogel matrix. (a) Molecular illustration of the glucose-binding process that causes swelling of the hydrogel matrix. (b) Illustration of volumetric transition upon glucose introduction into or depletion from the glucose-sensitive hydrogel matrix.

The construction of such 3D-PBG hydrogel sensors requires nonionic hydrogel precursors to avoid disordering in the charge-stabilized 3D polystyrene particles.[24] These 3D crystalline colloidal array particles were fabricated by self-assembly and this process lasts 2 weeks which is time-consuming. 3D-IOs structure from templates have also been transferred to the hydrogel during the polymerization of monomers—once polymerized, the 3D-IOs were removed by chemical etching, yielding a periodic porous polymer.[30] The 3D-IO method also suffers from the high defect density and prone to damage during template etching. A limited range of detection is also a significant drawback of 3D-PBG hydrogel sensors.

1D-PBG hydrogel glucose sensors have been fabricated based on the diffusion of the silver nanoparticle in the glucose-responsive hydrogels, followed by laser treatment to form composite layers separated by hydrogel layers modulating the refractive index in one dimension.[31] The fabrication of the 1D-PBG sensor process requires many stages and these sensors also have a limited field of view, making readouts very complicated. 2D-PBG sensors based on colloidal crystal arrays (CCA) have also been realized.[14] Although these sensors were sensitive to glucose in the physiological concentration range, they had limitations in their fabrication.[32] These sensors require a well-ordered monolayer of particles, demanding optimization, and functionalization with phenylboronic acid postpolymerization.[10] In addition, readout requires setups of expensive optical fibers fixed on rotating stages, dark rooms and spectrophotometers connected to a computer. Consequently, the PBG sensors could not find their way into low-cost mass production and point of care. Table S1 presentsa comparison of various types of glucose sensors summarizing the working principle, advantages, disadvantages, and detection ranges.

In this work, we developed a glucose sensor that achieves the crucial need of fast and economical fabrication process and a simple readout method. We introduced a transducer (holographic optical diffusing microstructures) that was easy to imprint on the surface of the glucose-responsive hydrogel through the UV gel curing process, facilitating and accelerating the fabrication process. The volumetric change of the hydrogel in response to various glucose concentrations modulated the dimensions of the optical diffusing microstructures and hence the scattering efficiency of the sensor. As a result, the beam profile and power for the transmitted and reflected beams changed. The readouts were taken using an optical powermeter and also with a smartphone app, exploiting the smartphone's ambient light sensor. Therefore, this sensor offers advantages in terms of its fast and facile preparation and simple readouts within physiological ranges.

RESULTS AND DISCUSSION

A holographic diffuser was mirror replicated on the hydrogel network during photopolymerization (Figure 2). Optical microscopy images confirmed successful transfer of the mirror-replicated structure on the hydrogel layer. Both the holographic diffuser and hydrogel sensor were illuminated with broadband white light and laser beam (λ = 532 nm). The

DOI: 10.1021/acsnano.7b07082
ACS Nano 2018, 12, 2283−2291

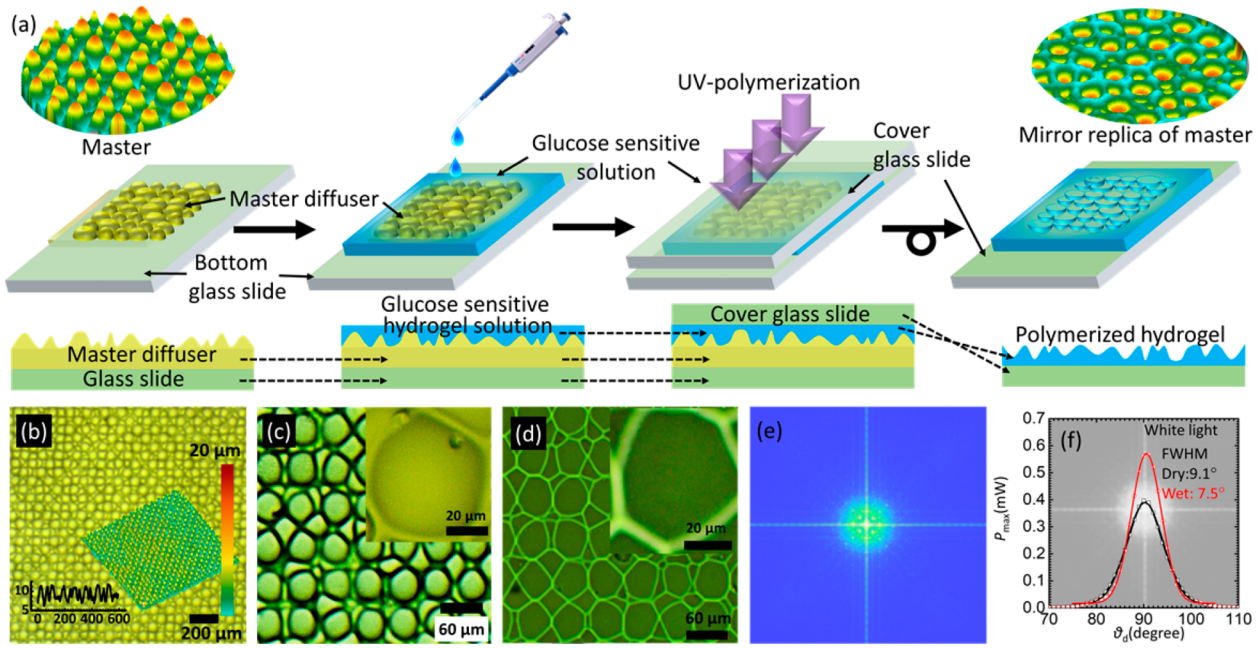

Figure 2. Microimprinting of holographic diffusers in hydrogel films. (a) Schematic for the fabrication process of hydrogel-based optical glucose sensor: a diffuser master replica is drop-cast with a glucose-sensitive solution which is polymerized using UV light. After polymerization, the master stamp is removed, and the imprinted glucose-sensitive hydrogel is obtained on the glass slide. (b–d) Microscopic images of the master diffuser and hydrogel. (e) Theoretically obtained Fourier transform of the diffuser giving the profile of the diffused light spot after interacting with glucose molecules. (f) Diffused light profile after the broadband white light is transmitted through the sensor in ambient (40% humidity) and fully hydrated conditions.

holographic diffuser exhibited a wider divergence/diffusion angles, $\Delta\theta_d \sim 40°$ and 35° for both broadband white light and monochromatic beams, respectively, as compared to the angles, $\Delta\theta_d \sim 20°$ and 15°, respectively, obtained for the imprinted hydrogel matrix. In addition, the maximum transmitted light intensity detected by using a photodetector for the holographic diffuser was ~2 times lower than that of the imprinted hydrogel matrix. The holographic master had a higher divergence, which allowed lesser light (luminance) to reach the photodetector placed at the identical distance as compared to its mirror replica of the hydrogel matrix. The difference in θ_d was expected because of the difference in the selection of materials and fabrication processes between the holographic diffuser and the imprinted hydrogel matrix.

The light dispersion properties of the imprinted hydrogel matrix weakened when it was exposed to the highly humid conditions. In fully hydrated conditions, the hydrogel matrix exhibited a smaller θ_d angle and higher maximum transmitted power than that of 40% relative humidity conditions (Figure 2f). The optical hydrogel matrix as a sensor swelled upon partial or full hydration, causing an initial size increase in the structural profile of the replicated microstructure. This change decreased the sensor's diffusive properties and, consequently, the divergence angle. Furthermore, the index matching effect due to the introduction of water on the surface decreased the roughness and also waveguided the transmitted light inline to the direction of the incident beam and reduced the beam divergence. Therefore, the decrease in the spot size in the case of full hydration increased the intensity maxima of the transmitted light when recorded at the center of the spot. For subsequent experiments, the sensor's reference was set according to its fully hydrated condition. The scattering profile of the holographic diffuser and the optical hydrogel sensor were similar for the blue, green, and red laser beam illumination (Figure S3).

Microimprinted hydrogel sensors were tested in different glucose concentrations in transmission mode using monochromatic light (Figure 3). The sensing was carried out by measuring the transmitted light intensity and recording the profile/diameter of the diffused light after passing through the optical hydrogel sensor (Figure 3c–e). The sensor was equilibrated in PBS solution (pH 7.4, ionic strength = 150 mM, 24 °C) for 2 h, and each measurement for different glucose concentration (M) within the range $0 \leq M \leq 100$ mM was carried out after 90 min to the last preceding sensing trial. An incident monochromatic light beam of λ = 532 nm was used, and sensing measurements were performed in the transmission mode. Figure 3a illustrates the schematic of the experimental setup in sensing experiments. In addition to the swelling caused by water diffusion inside the optical hydrogel sensor, glucose swelled the sensor due to the formation of anionic boronate–glucose 1:1 complexation in the hydrogel matrix that increased the boronate anions, leading to increasing Donnan osmotic pressure and, hence, caused a positive volumetric shift. For low pH solutions (pH < pK_a), the phenylboronic acid existed in uncharged trigonal configuration. It complexes with glucose-forming boronate ester, which is far more acidic than the boronic acid.[33,34] The pK_a of the boronic ester is less than the pH of the solution (7.4), resulting in dissociation of the boronic ester donating a proton forming a stable boronate anion. For high pH solutions (pH > pK_a) the PBA existed in a stable and charged tetrahedral configuration that complexes with glucose to form boronate anion (Figure S4).[33,34] The dimensional shift in the imprinted microlenses on the sensor's surface altered the overall divergence of the beam by changing the focal length of each individual microlens. Figure 3b shows the working principle of the sensor. The

DOI: 10.1021/acsnano.7b07082
ACS Nano 2018, 12, 2283–2291

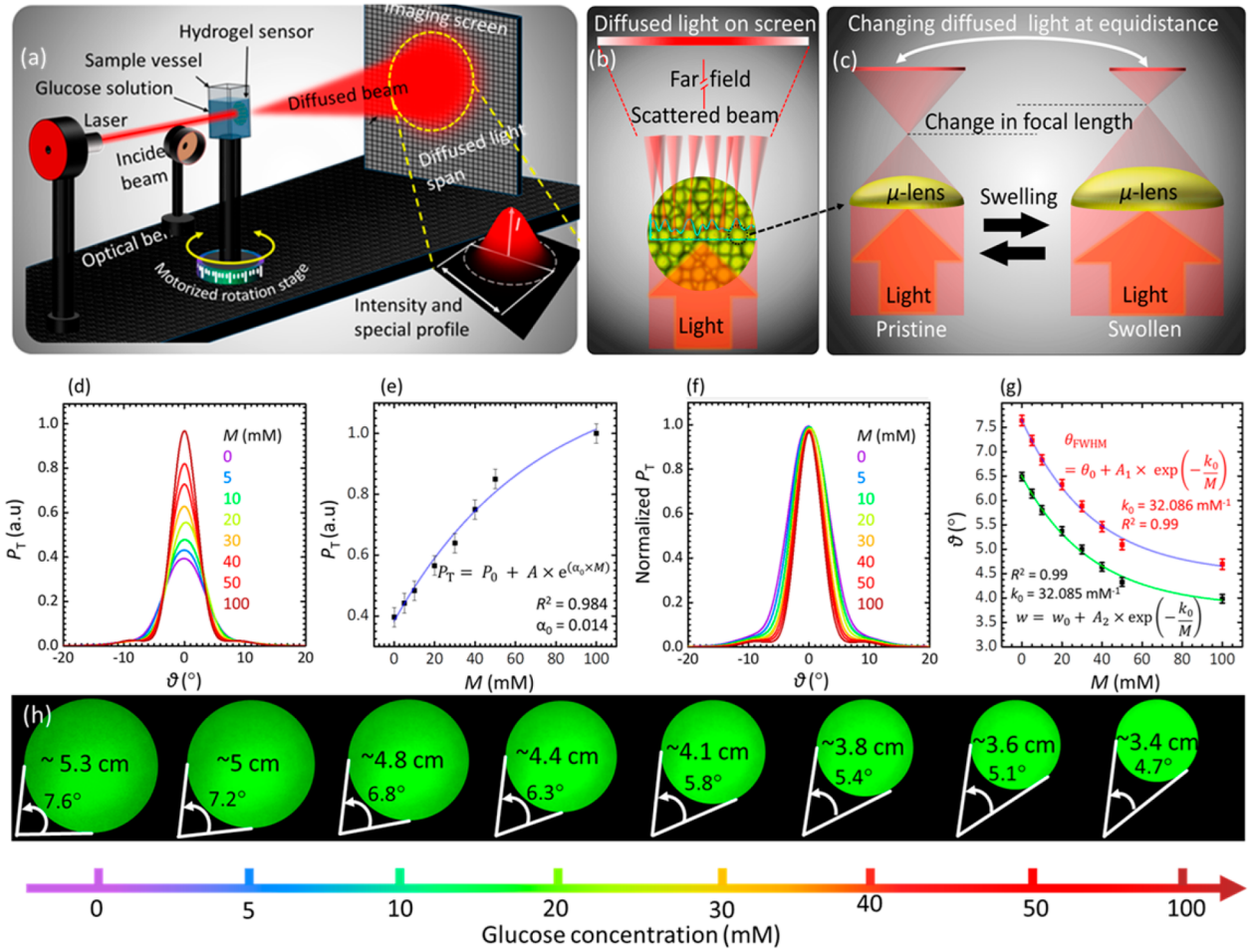

Figure 3. Quantification of glucose concentrations with an imprinted differ based hydrogel sensor. (a) Schematic of the monochromatic light transmission setup used to measure the optical response of the hydrogel sensor based on a diffuser structure when exposed to glucose. (b) Working principle of the diffuser, which is based on arrays of distorted microlenses−glucose binding alters the dimension of the microlenses and hence the profile of the transmitted light. (c) Transmitted light power, *P*, behavior for the green laser beam *versus* the diffusion angle for glucose concentration within the range 0 ≤ M ≤ 100 mM. (d) Peak transmitted light power, P_{max}, as a function of glucose concentration for 0 ≤ M ≤ 100 mM. (e) Normalized transmitted light power for different glucose concentrations *versus* the diffusion angle showing the change in the diameter of the diffused spot (captured on imaging screen). (f) Normalized P_T−θ_d plot. (g) Exponential fit for the fwhm and *w* conceived from (c). (h) Photographs of diffused monochromatic light spots after passing through the sensor submerged in different glucose concentration solutions. The diameter was restricted at fwhm of the transmitted power.

changing optical parameters could be correlated to the variation in the glucose concentration.

Increasing glucose concentration initially increased the maximum transmitted light power, P_{Tmax}, and shrank the diameter of the diffused light spot on the imaging screen (Figure 3d−h). Upon increasing the glucose concentration, 0 ≤ M ≤ 100 mM, the maximum transmitted light power P_{Tmax} and the diameter underwent a slower corresponding shift; the sensor response was saturated at high concentrations, below which the response was fairly linear with percentage sensitivity of S ∼ 2.5% mM^{-1} (or ∼11 μW mM^{-1}) calculated using the slope of the P−M curve, given by $S = \Delta P/\Delta M$, where ΔP and ΔM are the change in the transmitted optical power and change in glucose concentration, respectively. The sensitivity of our diffuser-based sensor is around 18 times higher than the recently reported work; for the glucose concentration range of 0−100 mM, the diffuser sensor showed the change of 128% in the transmitted power compared to the 7% attenuation of the transmitted light in ref 35. The decrease in sensitivity and saturation at higher glucose concentrations was due to the decrease in the available boronate binding sites and decreasing elasticity of the hydrogel matrix that competed against the volumetric swelling process. However, this nonlinear behavior could be fit very accurately with an exponential trend with a correlation coefficient of R^2 = 0.99 and exponential coefficient of ∼32.08 mM^{-1}. The visual shift of the diffused spectra was also very clear, which could be seen by the naked eye (Figure 3h). For diabetic patients, the required readout rate of the sensor for the shift of glucose concentration from 8 to 15 mM is 0.078 $mM{\cdot}min^{-1}$.[35] According to swelling kinetics of the sensor when it is immersed in glucose concentration of 10 mM, the sensor provides a readout rate of 0.14 mM per min which is higher than the required speed. The blood contains fructose and lactate; both complex with PBA under physiological conditions.[33,34] However, the glucose concentrations in blood for healthy (3.9−6.9 mM) and diabetic (7.2−10 mM) people are much larger than fructose concentrations (0.008 ± 0.001 and 0.012 ± 0.0036 mM) as well as the lactate (0.36−0.75 mM) in both conditions, respectively.[35,36] Previous studies reported a minimal interference from fructose of 0.5% and 3.5%

DOI: 10.1021/acsnano.7b07082
ACS Nano 2018, 12, 2283−2291

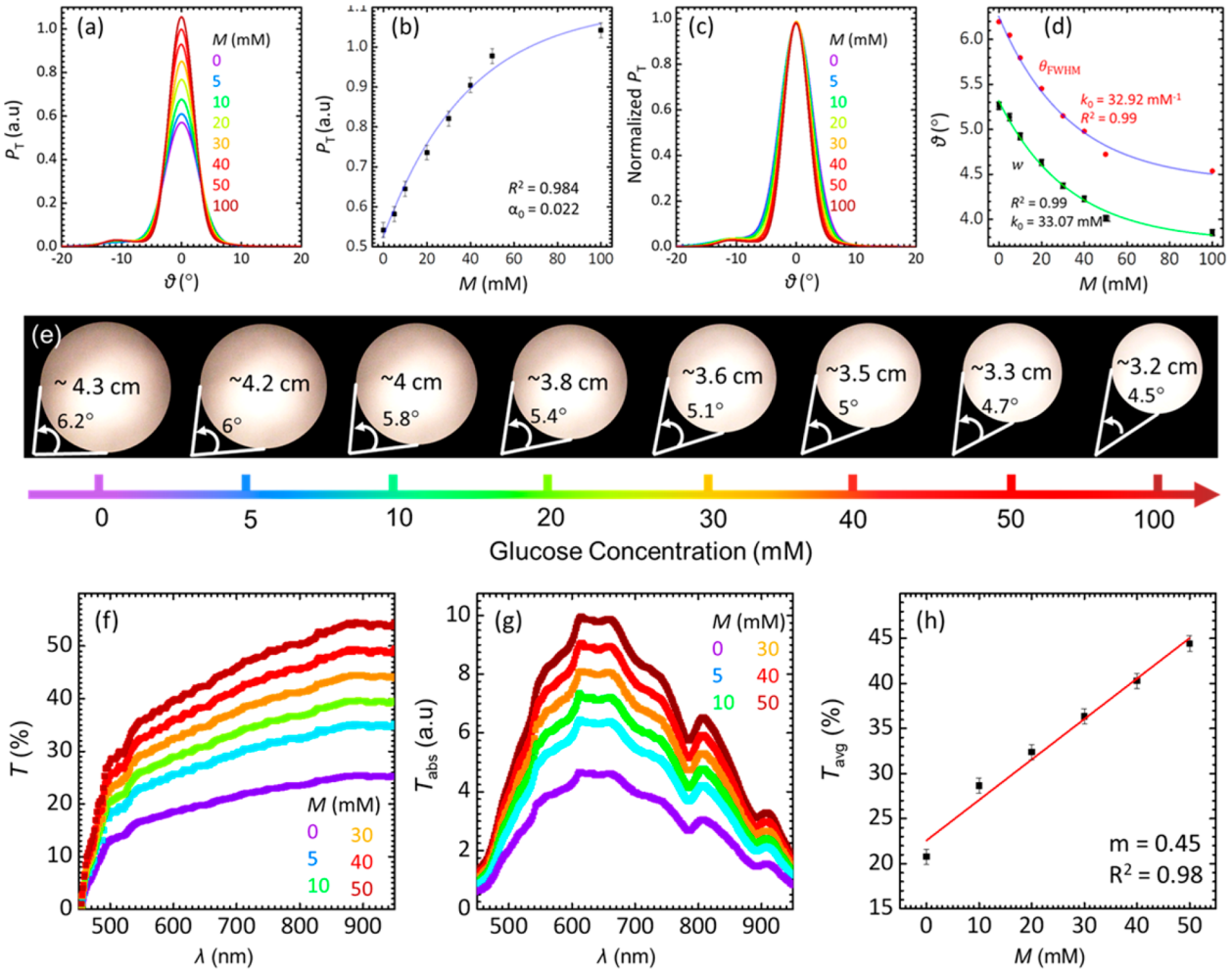

Figure 4. Quantification of glucose using the imprinted hydrogel sensor with a broadband light source for the concentration range of 0 ≤ M ≤ 100 mM. (a) P–θ_d trend of hydrogel sensor for different glucose concentrations. (b) P_{max} plotted against various glucose concentrations, M. (c) Normalized transmitted power of the broadband light *versus* the diffusion angle, showing the change in the diffused spot diameter with increasing glucose concentrations. (d) Exponential fit for the fwhm and w conceived from (c). (e) Photographs of diffused broadband light spots after passing through the sensor submerged in different glucose concentration solutions. The diameter was restricted at fwhm of the transmitted power. (f) Transmission spectra of the sensor for varying glucose concentration. (g) Absolute transmittance for increasing glucose concentration. (h) Average transmission of the sensor over 450−800 nm in various glucose concentrations.

for lactate for the glucose sensor that is prepared from same ingredients; PBA derivative and polymer matrix.[37]

Glucose concentration within the range of $0 \leq M \leq 100$ mM was also measured using broadband white light. Photographs of the diffused spots on a screen 40 cm away from the sensors were captured for visual detection. The divergence angle of the diffused light was consistent with the previous experiments carried out using the monochromatic light (Figure 4). An increase in the glucose concentration decreased the divergence angle and increased the power of the transmitted beam. The sensor response was linear for glucose concentrations within $0 \leq M \leq 50$ mM, and the sensor's sensitivity in this range was 11.6 μW·mM^{-1}. Parts f–h of Figure 4 show the transmitted light spectra of the glucose sensor. The sensor does not alter the spectral profile of the white light over the entire visible range. This means that the glucose detection can be performed reliably using any selective wavelength or the range of the wavelength due to the monotonic positive shift in the optical transmission against various glucose concentration. The diffuser-based sensor was able to quantify glucose within a wider detection range as compared to its other counterparts based on the visual detection scheme (1D and 3D PBG sensors).

The swelling dynamics of the sensor were studied for 10−50 mM glucose concentrations (Figure 5a–e). The spot profile and P_{max} were recorded at 6 min intervals. Upon exposure to glucose solution, the binding equilibrium reached to saturation in less than 60 min. This time was half of that reported in previous studies, where the saturation time for the 3PBA-modified PCCAs and holographic sensors was around 2 h.[12] The rapid response and quicker saturation time is an important step toward the practical implementation of such sensors. The quick response was due to the microengineered surface of the sensor that increases the active surface area and improved the diffusion rate of the glucose into the hydrogel matrix

The stability and reusability of the sensor were investigated by recording the response of the sensor for four complete cycles (Figure 5f). The sensor's response for glucose concentrations was measured for ∼100 min, followed by the reset using an acetate buffer of pH 4.6 for ∼10 s and then for ∼60 min in PBS buffer before commencing the next cycle for 10 mM glucose concentration. The increasing trend of P_{max}

DOI: 10.1021/acsnano.7b07082
ACS Nano 2018, 12, 2283−2291

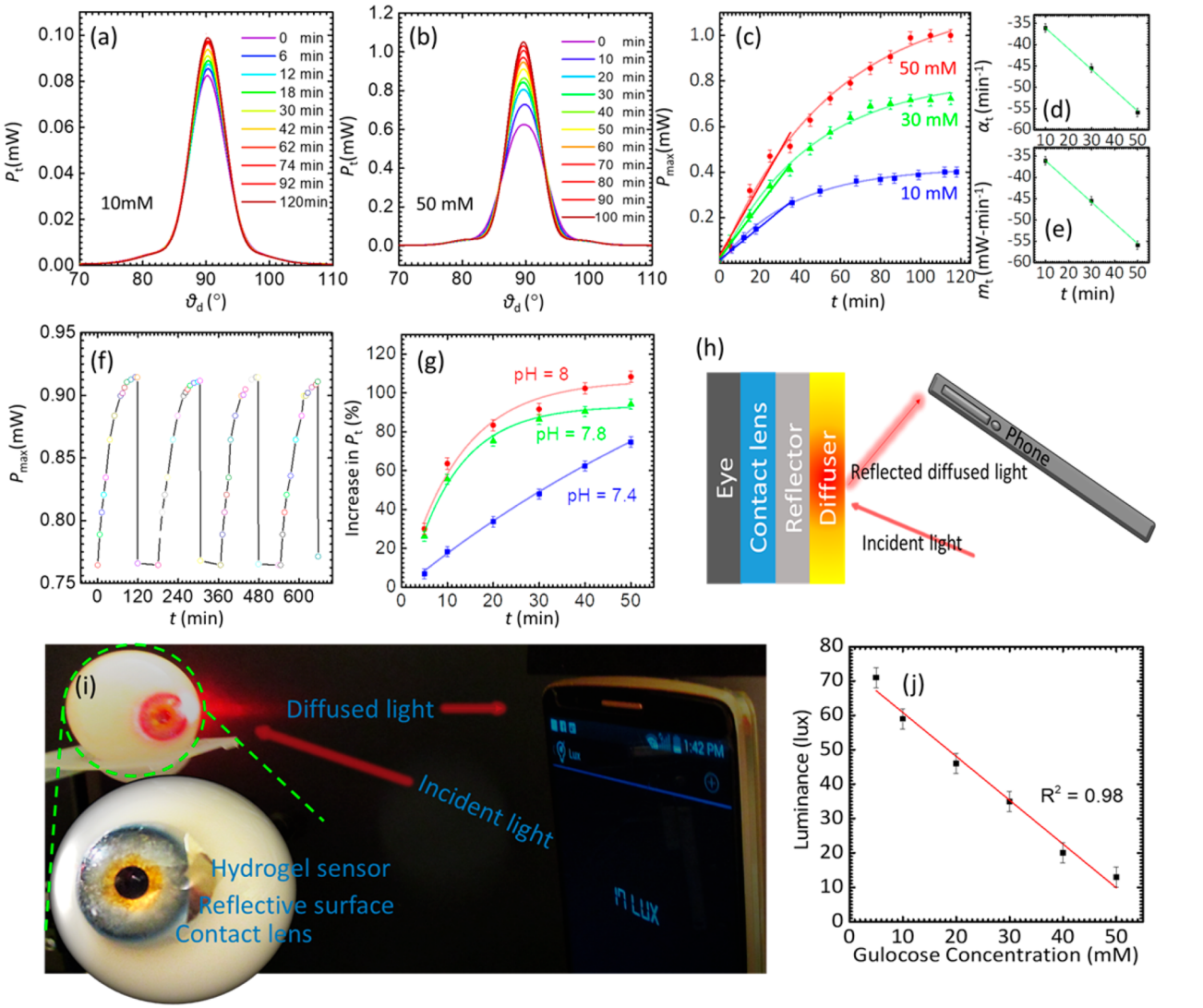

Figure 5. Reusability and response time of the imprinted optical glucose sensor. (a) Transmitted light power *versus* the diffusion angle recorded within the time span of $0 \leq t \leq 120$ min for 10 mM glucose concentration. (b) Optical transmitted power *versus* the diffusion angle recorded within the time span of $0 \leq t \leq 120$ min for 50 mM glucose concentration. (c) Peak power of the transmitted light *versus* 10, 30, and 50 mM glucose concentration over 120 min. (d, e) Time coefficients and slopes calculated using exponential fit (for at all data points) and linear fit for shorter span (over 40 min), respectively. (f) Switching of the sensor for various cycles against introduction or depletion of glucose (10 mM). (g) pH sensitivity of the hydrogel sensor for various glucose concentration at different pH values. (h) Schematic illustration of glucose sensing using a mobile phone. Microimprinted optical glucose sensor integrated on a contact lens. The light illuminated on the glucose sensor reflects back and alters the diffused light profile upon different glucose concentration exposures. (i) Experimental setup: photograph of an artificial eye with attached contact lens and sensor and schematic of the construction of contact lens. (j) Quantification of glucose sensing using a smartphone camera taken at a distance of 10 cm.

remained identical throughout experiments with the same saturation values for all the cycles. Similarly, the switching off behavior returned to the initial value quickly; the trend was unchanged throughout all the cycles. These results are important as our sensor exhibited reusability, no signal hysteresis or drift after each cycle, and identical sensitivity for each cycle. The effect of pH on the glucose detection was studied (Figure 5g). As shown in Figure 5, the sensitivity of the sensor increased with increasing pH. The highest sensitivity was recorded for pH 8, while at the physiological pH (7.4), a relatively lower glucose sensitivity was observed, consistent with the previous studies.[38,39] To explain the higher sensitivity of the sensor at higher pH values, the effect of pH on the sensor was examined (Figure S11). We found that upon increasing the pH from 4 to 6, the hydrogel slightly swells and consequently a slight increase in the transmitted power was recorded, indicating an inconsequential increase in the anionic boronate ions. The sensor exhibited a linear and higher response between the pH values of 6 and 9, as the concentrations of boronate ions increased significantly. Therefore, the higher sensitivity at higher pH glucose solutions might be due to an increase in the concentration of the anionic boronate ions which have high affinity to complexes with glucose forming a stable boronate anion. The sensitivity of the glucose sensor is not only affected by the pH of the glucose solution, but also by the ionic strength of the solution. It has been found that increasing the ionic strength of the aqueous solution increases the charged PBA in the polymer matrix raising up the Donnan potential, leading to the improved swelling response of the sensor.[22]

DOI: 10.1021/acsnano.7b07082
ACS Nano 2018, 12, 2283−2291

The thickness of the prepared glucose sensor was ~350 μm (Figure S2) as measured under an optical microscope. We could not use samples of thickness <350 μm as handling limitations of our free-standing sensors became more severe below this thickness. It is known that thicker sensors provide higher sensitivity on account of the response and saturation times, which become longer.[39] We believe that reducing the thickness of the sensor to nanoscale would candidate the sensor for real-time monitoring as the response and saturation times of the sensor would be within a few seconds. The transduction mechanism used to monitor the volumetric modulation is also an important factor that affects the sensitivity; for example, a 2.5 D photonic structure based sensor showed a quick response time, but the transduction mechanism posed the lowest sensing limit to ~10 mM.[40]

The effect of glucose complexation with the immobile PBA in the hydrogel matrix on the mechanical properties has been studied (Figure S9). The elasticity/Young's modulus for the sensor in absence of glucose was ~175 kPa and increased to ~218 kPa for the glucose concentration of 50 mM. The stiffness of the sensor increased from ~0.49 to 0.61 N/m, indicating a decrease in the flexibility. Increasing the sensor stiffness with glucose complexing may also explain the decreased sensitivity of the sensor at high glucose concentrations.

To show the utility of the sensor, we attached it on a small reflective sheet and incorporated on a contact lens (Figure 5h–j). Light intensity measurements were obtained in the reflection mode (with the incident and reflection angles of 45° with respect to the normal) using a smartphone photodiode. The inbuilt light sensor in the smartphone was utilized to capture the backscattered light (at a distance of 12 cm) and record its luminance. For this purpose, we used the "Smart Tools" android app which is freely available from the Google app store. Upon continuous application of different glucose solutions on the sensor surface, the changing luminance against varying glucose concentration (0–50 mM) was measured. The sensor was sensitive to the glucose concentration in the range of 5 mM and upward. The sensitivity of such sensors and thickness are inversely proportional. We anticipate that the sensitivity will improve to work in the tear range (0.26–0.9) with further optimization to the sensor's thickness and decreasing the resolution of the diffusing microstructures. These modifications can improve the sensor's active surface area and as a result, minimal swelling of the sensor will alter the transmitted and reflected beam profile.[41] Although, tear constituents such as fructose and lactate may interfere with the glucose measurements, this can be resolved by developing a highly glucose-selective bis-boronic acid functionalized hydrogel.

We anticipate no harm of illuminating the eyes for few seconds with a white light source as the ophthalmologists examine the patient's eyes by ophthalmoscopes that are provided by light pointers. The data file can be stored in ASCII format for global recognition and can be remotely sent to the physician for better health and care facilities. In contrast to other sophisticated electrochemical sensing schemes for glucose sensing, optical sensors incorporated in contact lenses do not require an electrical powersupply, significantly simplifying the operation and readout system with already available CMOS photodiode light sensors in smartphones.[42]

CONCLUSION

We have demonstrated an optical glucose sensor based on a diffuser architecture in a contact lens. The diffuser structure was initially mirror-replicated onto a glucose-sensitive hydrogel. The structure of the diffuser was based on microengineered lens arrays that exhibited a focal length modulation in response to the overall size modification of the hydrogel upon exposure to different glucose concentrations. Consequently, the changing focal lengths changed the diffused light profile being transmitted or reflected from the surface of the sensor, thereby changing the light intensity of the diffused spot within a given transmission area. This change was measured as a function the glucose concentration with the range of 0 to 100 mM. The sensor was sensitive to glucose well within the physiological conditions. More importantly, this optical sensor can be adapted as a minimally invasive real-time measurement method as important when finger prick blood sampling in glucose measurements at point-of-care settings is associated low patient compliance. The developed sensor was also reversible and reusable and exhibited no signal drift and hysteresis over multiple cycles or glucose concentration increase and depletion. We have successfully demonstrated such sensing using a hydrogel diffuser-based glucose sensor embedded in a contact lens and tested it on an artificial eye. Our proof-of-concept technology may be vital for chronic diseases cases, especially for type 1 diabetics, where continuous glucose monitoring is an important necessity for blood glucose management at point-of-care settings.

METHODS

Acrylamide (AA), *N*,*N*′-methylenebis(acrylamide) (BIS), 3-(acrylamido) phenylboronic acid (3-APBA), dimethyl sulfoxide (DMSO), 2,2-diethoxyacetophenone (DEAP), β-D-(+)-glucose, and phosphate-buffered saline (PBS) were purchased from Sigma-Aldrich and used without further purification. The acrylamide hydrogel film was synthesized by the free-radical polymerization utilizing DEAP as the photoinitiator and BIS as the cross-linker. The monomer solution was prepared from AA (78.5 mol %), BIS (1.5 mol %), 3-APBA (20 mol %), DEAP, and DMSO. The suspended monomer solution was stir-mixed for 10 min at 24 °C. Prepolymer solution (100 μL) was dropcast directly onto a master stamp surface based on a laser microengineered diffuser structure. A hydrophobic glass slide was placed on top the solution to obtain a uniform thickness. A photopolymerization process was initiated with a UV amp (Black Ray, 365 nm) for 5 min. A holographic diffuser was mirror replicated on the hydrogel network during photopolymerization. Subsequently, the resulting replica hydrogel was peeled off the master stamp, washed with deionized water, and kept in the dry condition prior to further experiments. One of the advantages of the diffuser sensor is the one-step preparation—that is, acrylamide, the cross-linker, and PBA are mixed together in the initiator solution followed by a single UV-assisted cross-linking process. In this method, the immobilized amount of PBA in the polymer is as same as the amount we added to the monomer solution which was 20% mol of the mixed monomer. The single-step method virtually gives a complete loading of the added PBA. This strategy is different compared to other coupling methods, where, polymerization of the acrylamide is carried out first, followed by the attachment of PBA using EDC. In this method, the encapsulation of poly acrylamide is done in the solution containing PBA and EDC for certain time duration. The loaded amount of phenylboronic acid to the polyacrylamide depends on the time span for the encapsulation process and initial concentration of PBA in the solution.

The thickness and surface of the holographic diffuser and the prepared hydrogel sensor were investigated using an optical microscope (Zeiss, 5× and 20× objective lens). For optical characterization, the setup comprised of two inline rotational stages (Thorlab), one

DOI: 10.1021/acsnano.7b07082
ACS Nano 2018, 12, 2283–2291

containing a 3D translational stage (Thorlab) with a sample holder and the other with the light source mount, and an optical power meter located at 12 cm from the sensor, all fixed on an optical bench. The master stamp and optical sensor were illuminated by monochromatic and broadband light sources at their normal and the transmitted diffused light spot were scanned by an optical power meter (Thorlabs, PM100A) for different sample orientations. The beam profile of the transmitted light was also studied using an imaging screen setup (by replacing the optical power meter with an imaging screen). To measure the response of the optical hydrogel sensor against the variation in glucose concentrations, the hydrogel was equilibrated in PBS buffer (7.4 pH, 24 °C, ionic strength = 150 mM) for 2 h, and optical transmission experiments were repeated under physiological conditions for different glucose concentrations. The sensing was also carried out on a sensor-integrated contact lens on an artificial eye by obtaining readouts with a smartphone camera and app, and results were compared with data recorded with the optical power meter.

ASSOCIATED CONTENT

Supporting Information

The Supporting Information is available free of charge on the ACS Publications website at DOI: 10.1021/acsnano.7b07082.

Comparison table for various glucose sensors in the literature; results on the cross-section of the sensor under an optical microscope, the stiffness of the sensor with and without glucose complexation, effect of pH on the sensor performance, and schematic diagram for the PBA complexation with glucose (PDF)

AUTHOR INFORMATION

Corresponding Authors

*E-mail: mie604@bham.ac.uk. Tel: +441214158623.
*E-mail: h.butt@bham.ac.uk. Tel: +441214158623.

ORCID

Ali K. Yetisen: 0000-0003-0896-267X

Author Contributions

M.E. and H.B. conceived the project idea. M.E. designed the project, carried out experiments, analyzed results, and wrote the article. M.U.H. performed the contact lens and mobile phone experiments and helped with manuscript preparation. H.B. supervised experiments and led the project. A.K.Y. revised the manuscript and provided intellectual contributions throughout the project.

Notes

The authors declare no competing financial interest.

ACKNOWLEDGMENTS

We thank the Wellcome Trust and the Leverhulme Trust for research funding. We thank Prof. Arshad Bhatti (Department of Physics, COMSATS Institute of Information Technology) for useful discussions.

REFERENCES

(1) He, H.; Xu, X.; Wu, H.; Jin, Y. Enzymatic Plasmonic Engineering of Ag/Au Bimetallic Nanoshells and Their Use for Sensitive Optical Glucose Sensing. *Adv. Mater.* **2012**, *24*, 1736−1740.

(2) Aslan, K.; Lakowicz, J. R.; Geddes, C. D. Nanogold-Plasmon-Resonance-Based Glucose Sensing. *Anal. Biochem.* **2004**, *330*, 145−155.

(3) Le Ru, E.; Etchegoin, P. *Principles of Surface-Enhanced Raman Spectroscopy: And Related Plasmonic Effects*; Elsevier, 2008.

(4) Gupta, V. K.; Atar, N.; Yola, M. L.; Eryılmaz, M.; Torul, H.; Tamer, U.; Boyacı, İ. H.; Üstündağ, Z. A Novel Glucose Biosensor Platform Based on Ag@ Aunps Modified Graphene Oxide Nanocomposite and Sers Application. *J. Colloid Interface Sci.* **2013**, *406*, 231−237.

(5) Al-Ogaidi, I.; Gou, H.; Al-Kazaz, A. K. A.; Aguilar, Z. P.; Melconian, A. K.; Zheng, P.; Wu, N. A Gold@ Silica Core−Shell Nanoparticle-Based Surface-Enhanced Raman Scattering Biosensor for Label-Free Glucose Detection. *Anal. Chim. Acta* **2014**, *811*, 76−80.

(6) Hu, Y.; Cheng, H.; Zhao, X.; Wu, J.; Muhammad, F.; Lin, S.; He, J.; Zhou, L.; Zhang, C.; Deng, Y. Surface-Enhanced Raman Scattering Active Gold Nanoparticles with Enzyme-Mimicking Activities for Measuring Glucose and Lactate in Living Tissues. *ACS Nano* **2017**, *11*, 5558−5566.

(7) Badugu, R.; Lakowicz, J. R.; Geddes, C. D. Noninvasive Continuous Monitoring of Physiological Glucose Using a Monosaccharide-Sensing Contact Lens. *Anal. Chem.* **2004**, *76*, 610−618.

(8) Alexeev, V. L.; Sharma, A. C.; Goponenko, A. V.; Das, S.; Lednev, I. K.; Wilcox, C. S.; Finegold, D. N.; Asher, S. A. High Ionic Strength Glucose-Sensing Photonic Crystal. *Anal. Chem.* **2003**, *75*, 2316−2323.

(9) Cobo, I.; Li, M.; Sumerlin, B. S.; Perrier, S. Smart Hybrid Materials by Conjugation of Responsive Polymers to Biomacromolecules. *Nat. Mater.* **2015**, *14*, 143−159.

(10) Culver, H. R.; Clegg, J. R.; Peppas, N. A. Analyte-Responsive Hydrogels: Intelligent Materials for Biosensing and Drug Delivery. *Acc. Chem. Res.* **2017**, *50*, 170−178.

(11) Alexeev, V. L.; Das, S.; Finegold, D. N.; Asher, S. A. Photonic Crystal Glucose-Sensing Material for Noninvasive Monitoring of Glucose in Tear Fluid. *Clin. Chem.* **2004**, *50*, 2353−2360.

(12) Yetisen, A. K.; Montelongo, Y.; da Cruz Vasconcellos, F.; Martinez-Hurtado, J.; Neupane, S.; Butt, H.; Qasim, M. M.; Blyth, J.; Burling, K.; Carmody, J. B. Reusable, Robust, and Accurate Laser-Generated Photonic Nanosensor. *Nano Lett.* **2014**, *14*, 3587−3593.

(13) Yetisen, A. K.; Butt, H.; da Cruz Vasconcellos, F.; Montelongo, Y.; Davidson, C. A.; Blyth, J.; Chan, L.; Carmody, J. B.; Vignolini, S.; Steiner, U. Light-Directed Writing of Chemically Tunable Narrow-Band Holographic Sensors. *Adv. Opt. Mater.* **2014**, *2*, 250−254.

(14) Huang, J.; Hu, X.; Zhang, W.; Zhang, Y.; Li, G. Ph and Ionic Strength Responsive Photonic Polymers Fabricated by Using Colloidal Crystal Templating. *Colloid Polym. Sci.* **2008**, *286*, 113−118.

(15) Ilavský, M.; Hrouz, J. Phase Transition in Swollen Gels. *Polym. Bull.* **1982**, *8*, 387−394.

(16) Slaughter, B. V.; Blanchard, A. T.; Maass, K. F.; Peppas, N. A. Dynamic Swelling Behavior of Interpenetrating Polymer Networks in Response to Temperature and Ph. *J. Appl. Polym. Sci.* **2015**, DOI: 10.1002/app.42076.

(17) Barry, R. A.; Wiltzius, P. Humidity-Sensing Inverse Opal Hydrogels. *Langmuir* **2006**, *22*, 1369−1374.

(18) Yetisen, A.; Qasim, M.; Nosheen, S.; Wilkinson, T.; Lowe, C. Pulsed Laser Writing of Holographic Nanosensors. *J. Mater. Chem. C* **2014**, *2*, 3569−3576.

(19) Katayama, S.; Hirokawa, Y.; Tanaka, T. Reentrant Phase Transition in Acrylamide-Derivative Copolymer Gels. *Macromolecules* **1984**, *17*, 2641−2643.

(20) Kabilan, S.; Marshall, A. J.; Sartain, F. K.; Lee, M.-C.; Hussain, A.; Yang, X.; Blyth, J.; Karangu, N.; James, K.; Zeng, J. Holographic Glucose Sensors. *Biosens. Bioelectron.* **2005**, *20*, 1602−1610.

(21) Zhao, Z. B.; Li, H.; Lu, Q. L.; Li, Y. L.; Jiang, Y. Multifunctional Sensors Based on Silicone Hydrogel and Their Responses to Solvents, Ph and Solution Composition. *Polym. Int.* **2017**, *66*, 566−572.

(22) Xue, F.; Meng, Z.; Wang, F.; Wang, Q.; Xue, M.; Xu, Z. A 2-D Photonic Crystal Hydrogel for Selective Sensing of Glucose. *J. Mater. Chem. A* **2014**, *2*, 9559−9565.

(23) Xu, J.; Yan, C.; Liu, C.; Zhou, C.; Hu, X.; Qi, F. Photonic Crystal Hydrogel Sensor for Detection of Nerve Agent. *IOP Conf. Ser.: Mater. Sci. Eng.*; IOP Publishing: Sanya, China, 2017; p 012024.

(24) Lee, Y.-J.; Pruzinsky, S. A.; Braun, P. V. Glucose-Sensitive Inverse Opal Hydrogels: Analysis of Optical Diffraction Response. *Langmuir* **2004**, *20*, 3096−3106.

(25) Hao, N.; Zhang, X.; Zhou, Z.; Qian, J.; Liu, Q.; Chen, S.; Zhang, Y.; Wang, K. Three-Dimensional Nitrogen-Doped Graphene Porous Hydrogel Fabricated Biosensing Platform with Enhanced Photo-

DOI: 10.1021/acsnano.7b07082
ACS Nano 2018, 12, 2283−2291

electrochemical Performance. Sens. *Sens. Actuators, B* **2017**, *250*, 476–483.
(26) Sabouri, A.; Yetisen, A. K.; Sadigzade, R.; Hassanin, H.; Essa, K.; Butt, H. Three-Dimensional Microstructured Lattices for Oil Sensing. *Energy Fuels* **2017**, *31*, 2524–2529.
(27) Ahmed, R.; Yetisen, A. K.; Yun, S. H.; Butt, H. Color-Selective Holographic Retroreflector Array for Sensing Applications. *Light: Sci. Appl.* **2017**, *6*, No. e16214.
(28) Asher, S. A.; Holtz, J.; Liu, L.; Wu, Z. Self-Assembly Motif for Creating Submicron Periodic Materials. Polymerized Crystalline Colloidal Arrays. *J. Am. Chem. Soc.* **1994**, *116*, 4997–4998.
(29) Nakayama, D.; Takeoka, Y.; Watanabe, M.; Kataoka, K. Simple and Precise Preparation of a Porous Gel for a Colorimetric Glucose Sensor by a Templating Technique. *Angew. Chem.* **2003**, *115*, 4329–4332.
(30) Honda, M.; Kataoka, K.; Seki, T.; Takeoka, Y. Confined Stimuli-Responsive Polymer Gel in Inverse Opal Polymer Membrane for Colorimetric Glucose Sensor. *Langmuir* **2009**, *25*, 8349–8356.
(31) Kabilan, S.; Blyth, J.; Lee, M.; Marshall, A.; Hussain, A.; Yang, X. P.; Lowe, C. Glucose-Sensitive Holographic Sensors. *J. Mol. Recognit.* **2004**, *17*, 162–166.
(32) Tavakoli, J.; Tang, Y. Hydrogel Based Sensors for Biomedical Applications: An Updated Review. *Polymers* **2017**, *9*, 364.
(33) Hisamitsu, I.; Kataoka, K.; Okano, T.; Sakurai, Y. Glucose-Responsive Gel from Phenylborate Polymer and Poly (Vinyl Alcohol): Prompt Response at Physiological pH through the Interaction of Borate with Amino Group in the Gel. *Pharm. Res.* **1997**, *14*, 289–293.
(34) Springsteen, G.; Wang, B. A Detailed Examination of Boronic Acid-Diol Complexation. *Tetrahedron* **2002**, *58*, 5291–5300.
(35) Yetisen, A. K.; Jiang, N.; Fallahi, A.; Montelongo, Y.; Ruiz-Esparza, G. U.; Tamayol, A.; Zhang, Y. S.; Mahmood, I.; Yang, S. A.; Kim, K. S., Glucose-Sensitive Hydrogel Optical Fibers Functionalized with Phenylboronic Acid. *Adv. Mater.* **2017**, *29*.160638010.1002/adma.201606380
(36) Engelgau, M. M.; Narayan, K.; Herman, W. H. Screening for Type 2 Diabetes. *Diabetes Care* **2000**, *23*, 1563–1580.
(37) Yetisen, A. K., Fundamentals of Holographic Sensing. *Holographic Sensors*; Springer: Cham, Switzerland, 2015; pp 27–51.
(38) Zhang, Y.; Guan, Y.; Zhou, S. Synthesis and Volume Phase Transitions of Glucose-Sensitive Microgels. *Biomacromolecules* **2006**, *7*, 3196–3201.
(39) Zhang, X.; Guan, Y.; Zhang, Y. Ultrathin Hydrogel Films for Rapid Optical Biosensing. *Biomacromolecules* **2012**, *13*, 92–97.
(40) Bajgrowicz-Cieslak, M.; Alqurashi, Y.; Elshereif, M. I.; Yetisen, A. K.; Hassan, M. U.; Butt, H. Optical Glucose Sensors Based on Hexagonally-Packed 2.5-Dimensional Photonic Concavities Imprinted in Phenylboronic Acid Functionalized Hydrogel Films. *RSC Adv.* **2017**, *7*, 53916–53924.
(41) Baca, J. T.; Finegold, D. N.; Asher, S. A. Tear Glucose Analysis for the Noninvasive Detection and Monitoring of Diabetes Mellitus. *Ocul. Surf.* **2007**, *5*, 280–293.
(42) Ul Hasan, K.; Asif, M. H.; Hassan, M. U.; Sandberg, M. O.; Nur, O.; Willander, M.; Fagerholm, S.; Strålfors, P. A Miniature Graphene-Based Biosensor for Intracellular Glucose Measurements. *Electrochim. Acta* **2015**, *174*, 574–580.

DOI: 10.1021/acsnano.7b07082
ACS Nano 2018, 12, 2283–2291